Throughput Maximization for Hybrid Backscatter Assisted Cognitive Wireless Powered Radio Networks

Bin Lyu, Haiyan Guo, Zhen Yang, and Guan Gui, *Senior Member, IEEE*

***Abstract*—In this paper, we consider a cognitive wireless powered communication network for Internet of Things applications, which consists of a primary communication pair and a secondary communication system. We propose a novel hybrid harvest-then-transmit (HTT) and backscatter communication (BackCom) mode for the information transmission of the secondary communication system. When the primary channel is busy, cognitive users (CUs) backscatter the incident signal from the primary transmitter to the information receiver in the ambient backscatter (AB) mode or harvest energy for the future information transmission. When the primary channel is idle, CUs backscatter the incident signal from the power beacon in the bistatic scatter (BS) mode or work in the HTT mode to transmit information. We further investigate the optimal time allocation between the AB mode and energy harvesting and that between the BS mode and the HTT mode for the sake of maximizing the throughput of the secondary communication system, and derive the numerical solutions. To be specific, we derive the closed-form optimal solution for a single CU case, and moreover, obtain the optimal combination of the working modes. Numerical results demonstrate the advantage of our proposed hybrid HTT and BackCom mode over the benchmark mode in terms of system throughput.**

***Index Terms*—Cognitive wireless powered communication network (CWPCN), harvest-then-transmit (HTT) mode, hybrid backscatter communication, throughput maximization.**

I. Introduction

THE EMERGING Internet of Things (IoT) is a network with billions of smart objects, where the objects are able to communicate and cooperate to facilitate our daily lives [1]–[3]. In recent years, IoT has been applied almost everywhere, such as agriculture, smart home, biomedicine, and public safety [4]. However, some key challenges still need to be addressed for the deployment of large-scale IoT, one of which is the limited network lifetime. It is because IoT devices are usually powered by their embedded batteries with small capacities, and replacing or recharging the batteries periodically is inconvenient especially when there are massive IoT devices [2].

Recently, energy harvesting (EH) has emerged as an effective energy supply for IoT devices, which can be used to significantly prolong the lifetime of IoT networks [5]. EH techniques enable IoT devices to scavenge energy from a lot of environmental sources, such as wind, thermal energy, and radio frequency (RF) signals. In particular, RF signals have recently drawn significant attention for powering IoT devices since they are stable and easy to control [4], [6], [7]. Inspired by this, RF-wireless power transfer (WPT) has been proposed for IoT. Moreover, the information transmission for IoT devices based on the harvested energy is also a key issue. Hence, based on RF-WPT, wireless powered communication networks (WPCNs), which are typically IoT networks applied in smart home, agriculture, etc., have recently been extensively studied [8]–[11].

Ju and Zhang [8] proposed the harvest-then-transmit (HTT) mode for the IoT network operation, where the energy-free IoT devices first harvest energy from the hybrid access point (HAP) and then use the harvested energy to transmit information to the HAP. Since the IoT devices do not have initial energy, the EH time for the HTT mode is always required, which may reduce the information transmission time. To improve the system performance, Ju and Zhang [9] extended the half-duplex WPCN in [8] to the full-duplex WPCN with the aid of two antennas at the HAP, where one antenna is employed for transmitting energy signals to the IoT devices and the other antenna is employed for receiving information signals from the IoT devices simultaneously. Considering that the IoT devices may suffer from the doubly near-far problem in a WPCN, Ju and Zhang [10] proposed the user cooperation scheme, in which the IoT device nearer to the HAP helps forward the far IoT device's information to the HAP, which improved the fairness among IoT devices. Chen *et al.* [11] proposed a harvest-then-cooperate mode, in which the energy-free IoT device and relay first harvest energy from the HAP and then work cooperatively for the information transmission. The proposed cooperation schemes in both [10] and [11] significantly improve the throughput of IoT networks.

Manuscript received December 30, 2017; revised February 28, 2018; accepted March 20, 2018. Date of publication March 28, 2018; date of current version June 8, 2018. This work was supported in part by the National Natural Science Foundation of China under Grant 61671252, Grant 61772287, and Grant 61471202, in part by the Jiangsu Distinguished Professor under Grant RK002STP16001, in part by the "1311 Talent Plan" of NUPT, in part by the Open Research Fund of the Key Laboratory of Ministry of Education in Broadband Wireless Communication and Sensor Network Technology under Grant JZNY201707, and in part by the Innovation Program of Graduate Education of Jiangsu Province under Grant KYLX15-0828. *(Corresponding authors: Zhen Yang; Guan Gui.)*

The authors are with the Key Laboratory of Ministry of Education in Broadband Wireless Communication and Sensor Network Technology, Nanjing University of Posts and Telecommunications, Nanjing 210003, China (e-mail: 13010511@njupt.edu.cn; guohy@njupt.edu.cn; yangz@njupt.edu.cn; guiguan@njupt.edu.cn).

Digital Object Identifier 10.1109/JIOT.2018.2820180

On the other hand, backscatter communication (BackCom) has attracted considerable attention for the communication between IoT devices without embedded energy supplies [12]–[14]. BackCom is operated by means of reflecting the incident signals rather than radiating signals actively via varying antenna impedance. Hence, the oscillators and analog-to-digital converters are not required for the generation of carrier signals and digital modulation, respectively, which significantly reduces circuit power consumption. This characteristic is applicable for IoT since it makes IoT devices keep alive easily. Moreover, BackCom does not need a long duration of EH comparing with the HTT mode. However, if the incident signals are not available, the IoT devices adopting the BackCom mode cannot communicate with each other. There are two popular modes of BackCom for IoT applications, which are bistatic scatter (BS) [12] and ambient backscatter (AB) [13], [14]. The BS mode requires a carrier emitter, which is suitable for the scenarios where the IoT devices have dedicated power sources, e.g., power beacons (PBs) [12]. While the AB mode exploits ambient RF signals, e.g., WiFi signals, as the incident signals [13], which is suitable for the scenarios that have some existing RF sources. Inspired by the advantages of BackCom, it is highly desirable to integrate BackCom in WPCNs to extend the IoT applications, for example, urgent data transmission and ubiquitous devices' connections [15]. Lyu *et al.* [16], [17] studied wireless powered heterogeneous networks, which include the IoT devices working in the HTT mode and the BackCom mode, respectively. In [18] and [19], a two-antenna HAP or the dislocated PB and information receiver (IR) were adopted in BackCom assisted WPCNs, respectively, to further improve the system throughput, where each IoT device works in either the BackCom mode or the HTT mode. Kim and Kim [20] proposed the hybrid BackCom mode for a WPCN, where the IoT devices choose the BS mode or the AB mode depending on their locations in the network.

The availability of spectrum is another challenge for IoT. As the number of IoT devices increases exponentially, it is not easy to allocate spectrum bands to these devices. Hence, equipping IoT devices with cognitive radio capability has been an important research direction [21]. Considering both the energy and spectrum limitations for IoT, Lee and Zhang [22] investigated a cognitive radio network (CRN) enabled secondary WPCN, termed cognitive WPCN (CWPCN), where the IoT devices in the secondary communication system, termed cognitive users (CUs), harvest energy not only from the HAP in the secondary system but also opportunistically from the primary transmitter (PT), and transmit information to the HAP with sharing the primary communication system's spectrum. In [23], an online energy management and spectrum management algorithm was designed in a CWPCN. Hoang *et al.* [24] applied BackCom in an overlay CWPCN, where the CU chooses the AB mode if the primary channel stays in the busy state and works in the HTT mode if the primary channel stays in the idle state. The optimal tradeoff between the AB and HTT modes was investigated to maximize the system throughput. Hoang *et al.* [25] extended the model in [24] to the multiple CUs scenario, which is more practical for IoT applications.

In this paper, we propose a hybrid HTT and BackCom (HTT-BackCom) mode in a CWPCN, where the secondary communication system is a wireless sensor network (WSN) for IoT. Compared with [24] and [25], each CU in our proposed model can work in both AB and BS modes such that we can fully exploit the PT and the PB to extend the information transmission duration, where the PT serves as the incident signal source for the AB mode and the PB is the incident signal source for the BS mode. Compared with [20], we assume that the choice between the AB and BS modes depends on the primary channel states. Moreover, the CUs need to share the spectrum with the primary communication pair such that the dedicated spectrum bands are not required. In our proposed hybrid HTT-BackCom mode, we consider a simplified interweave CRN, where the PT is active only for a fraction of time and its working state can be perfectly detected by the network [22].

The main contributions of this paper are summarized as follows. First, we propose a hybrid HTT-BackCom mode to exploit the advantages of both HTT and BackCom modes for IoT applications, which depends on the primary channel states, i.e., the busy state and the idle state. During the busy state, the AB mode is activated to backscatter the incident signal from the PT to the IR or the HTT mode is activated for dedicated EH. During the idle state, CUs adopt the BS mode to backscatter the incident signal from the PB or the HTT mode to transmit information to the IR. The proposed hybrid HTT-BackCom mode is shown to be a better way to solve the energy and spectrum limitations for IoT. Second, we study the throughput maximization problem of the secondary communication system by jointly investigating the optimal time tradeoff between the AB mode and EH and that between the BS mode and HTT mode. In particular, we derive the optimal solution in closed-form for a single CU case by exploiting the KKT conditions, which also shows the optimal combination of the CU's working modes. Third, we conduct numerical results to show the proposed hybrid mode with the optimal time allocation can significantly improve the throughput of the secondary communication.

The rest of this paper is organized as follows. In Section II, we give the system model. In Section III, we study the optimal time allocation problem to maximize the throughput of the secondary communication system. In Section IV, the benchmark scheme is analyzed. In Section V, we conduct numerical evaluations for the system performance. Finally, we provide conclusions in Section VI.

II. System Model

As illustrated in Fig. 1, we study a CWPCN consisting of a primary communication pair and a secondary communication system. The primary communication pair includes a PT (e.g., TV tower) and a primary receiver (PR). The secondary communication system, a WSN for IoT, consists of a PB, an IR, and K CUs (e.g., low-power IoT devices), denoted by $U_i, \forall i$. We assume that all terminals each has a single antenna. The CUs are typically placed nearer to the PB than the PT. The PT and the PB have stable energy supplies, while the CUs which

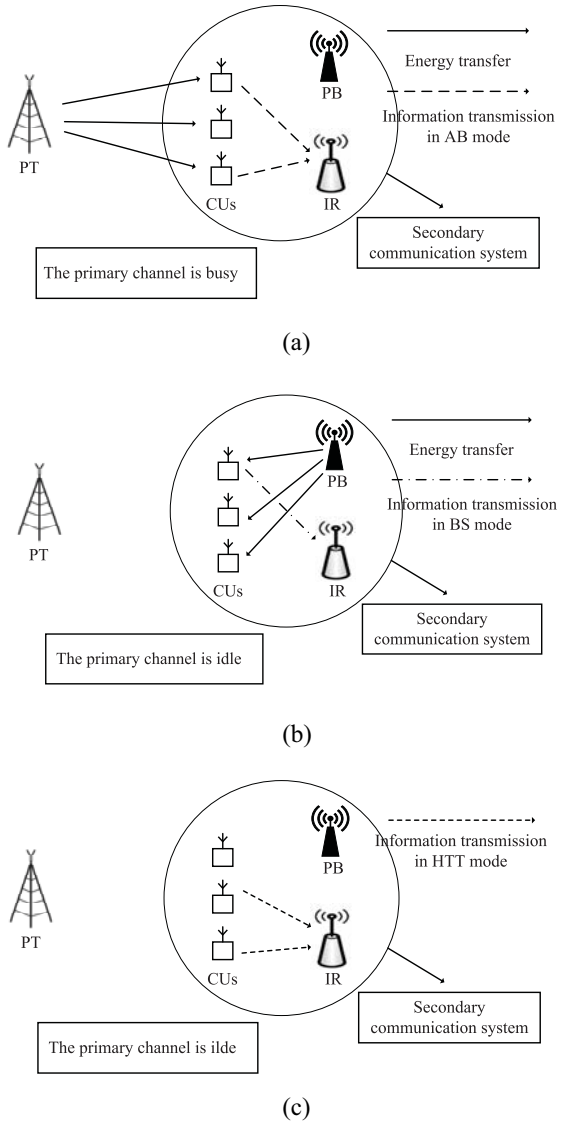

Fig. 1. CWPCN with hybrid BackCom. (a) CUs harvest energy from the PT or backscatter information in the AB mode. (b) CUs harvest energy from the PB or backscatter information in the BS mode. (c) CUs transmit information in the HTT mode.

do not have embedded energy sources need to be powered by the PT or the PB. Each CU works in either the HTT mode or the BackCom mode, but not simultaneously [26]. When the PT transmits signals to the PR, i.e., the primary channel stays in the busy state, the CUs can either harvest energy and store the harvested energy in their storages, or backscatter modulated signals to the IR. When the primary channel stays in the idle state, the PB is enabled to broadcast energy signals to the CUs, during which the CUs can also harvest energy or backscatter modulated signals. The harvested energy from both the PT and the PB is used for transmitting information signals to the IR.

The network is studied based on a time block with duration of T, the structure of which is illustrated in Fig. 2. Without loss of generality, we let $T = 1$. Denote the durations of the primary channel busy and idle periods as

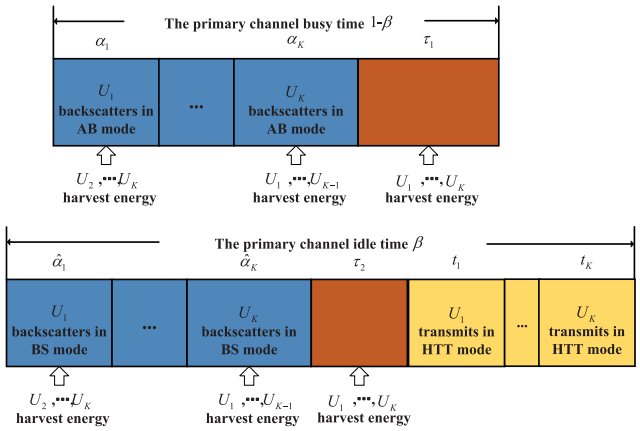

Fig. 2. Time block structure for a CWPCN.

$1-\beta$ and β, respectively.[1] We assume all CUs backscatter or transmit information via time division multiple access. If U_i stays in the BackCom mode to backscatter information to the IR, the other CUs can work in the HTT mode to harvest energy from the PT or the PB. Denote the time allocated to U_i's BackCom mode during the primary channel busy and idle periods as α_i and $\hat{\alpha}_i$, respectively. Moreover, during the primary channel busy and idle periods, the time slots with duration of τ_1 and τ_2 are, respectively, allocated to all CUs for harvesting energy. Hence, the total EH time of U_i during the channel busy and idle periods is given by $\sum_{j\neq i}\alpha_j + \tau_1$ and $\sum_{j\neq i}\hat{\alpha}_j + \tau_2$, respectively. During the primary channel idle period, the information transmission of the HTT mode is enabled. Denote the information transmission time of U_i as t_i. Since each CU only backscatters or transmits information to the IR during its allocated time slots, the information of each CU's working mode can be known by the IR such that the IR can apply the corresponding demodulators to extract useful information [24].

A. HTT Mode

The HTT mode consists of two phases, i.e., EH and information transmission phases. That is to say, the CUs first harvest energy from the PT or the PB, and then use the harvested energy to transmit information to the IR. Denote the channel power gains between the PT and U_i, between the PB and U_i, and between U_i and the IR as h_p^i, h_h^i, and g_h^i, respectively. We follow the Friis equation, h_p^i, h_h^i, and g_h^i are thus given by

$$h_p^i = \frac{G_p G_u \lambda_p^2}{\left(4\pi d_p^i\right)^2}$$

$$h_h^i = \frac{G_h G_u \lambda_h^2}{\left(4\pi d_h^i\right)^2}$$

[1]Note that the working states of the primary channel should be first detected via some advanced spectrum sensing techniques [22]. For example, the IR adopts the energy detection technique to detect the states of the primary channel and then forwards the sensing result to the CUs. Hence, the CUs can backscatter or transmit information based on the states of the primary channel.

$$g_h^i = \frac{G_u G_r \lambda_u^2}{\left(4\pi d_u^i\right)^2}$$

where G_p, G_h, G_u, and G_r are the antenna gains of the PT, the PB, U_i, and the IR, respectively, λ_p, λ_h, and λ_u are the signal wavelengths of the PT, the PB, and U_i, respectively, d_p^i, d_h^i, and d_u^i are the distances between the PT and U_i, between the PB and U_i, and between U_i and the IR, respectively.

During the EH phase, the harvested energy of U_i from the PT and the PB, denoted by E_p^i and E_h^i, are given by

$$E_p^i = \eta^i P_p h_p^i \left(\sum_{j\neq i}^{K} \alpha_j + \tau_1\right)$$
$$E_h^i = \eta^i P_h h_h^i \left(\sum_{j\neq i}^{K} \hat{\alpha}_j + \tau_2\right)$$

where P_p is the PT's transmit power, P_h is the PB's transmit power, η^i is the EH efficiency of U_i.

During the information transmission phase, U_i uses up its harvested energy to transmit information during t_i. Hence, the average transmit power of U_i is given by

$$P_t^i = \frac{E_p^i + E_h^i}{t_i}.$$

The information transmission bits of U_i in the HTT mode is given by

$$R_h^i = t_i W \log_2\left(1 + \frac{P_t^i g_h^i}{\sigma^2}\right) = t_i W \log_2\left(1 + \frac{\gamma_p^i\left(\sum_{j\neq i}^{K} \alpha_j + \tau_1\right) + \gamma_h^i\left(\sum_{j\neq i}^{K} \hat{\alpha}_j + \tau_2\right)}{t_i}\right) \quad (1)$$

where W is the bandwidth, σ^2 is the noise power at the IR, $\gamma_p^i = [(\eta^i P_p h_p^i g_h^i)/\sigma^2]$, and $\gamma_h^i = [(\eta^i P_h h_h^i g_h^i)/\sigma^2]$.

B. BackCom Mode

We consider a hybrid BackCom that includes two types, e.g., AB and BS modes. Different from the HTT mode, for BackCom, the CU reflects the instantaneous incident signal from the PT or the PB to the IR such that the dedicated EH phase is not required. During the primary channel busy period, the PT serves as the incident signal source. Since the PT is far from the CUs, the AB mode can be activated. In contrary, the PB is placed nearer to the CUs than the PT, and the BS mode can thus be activated during the primary channel idle period.

1) AB Mode: Recently, many prototypes of AB transmission have been proposed [13], [14]. Here, we utilize the prototype designed in [13]. In this prototype, when the incident signal is available at a CU, the antenna impedance is varied to achieve the information backscattering, and the simple on–off keying modulation is performed. It is reported that the backscatter rate is determined by the setting of the *RC* circuit elements [13]. Denote the backscatter rate of U_i in the AB mode as B_a^i, and the backscatter bits of U_i is thus given by

$$R_a^i = B_a^i \alpha_i. \quad (2)$$

Since the backscattered signal power is very low, AB is unregulated by FCC [27]. Following this policy, we do not consider the interference caused by the AB mode at the primary communication pair. Moreover, the CUs can also offset the carrier phase by a certain frequency to avoid the interference [28].

2) BS Mode: When the BS mode is activated at U_i, the binary frequency-shift keying (FSK) modulation is performed following [12]. It is obvious that the IR can receive the radiated signal from the PB and the backscattered signal from CUs. Following [20], we assume that IR has the sophisticated preprocessing function such that it can compensate the carrier frequency offset and remove the direct current part of the received signal before the detection of the backscattered FSK signal [12]. Hence, the received power at the IR is expressed as

$$P_b^i = P_h h_h^i g_h^i s^2 \left(\frac{\Gamma_0 - \Gamma_1}{2}\right)^2 \left(\frac{4}{\pi}\right)^2$$

where s is the tag scattering efficiency, Γ_0 and Γ_1 are the reflection coefficients [12], [20]. The achievable rate of the BS mode is thus given by

$$B_b^i = W \log_2\left(1 + \frac{\xi P_b^i}{\sigma^2}\right) \quad (3)$$

where ξ is the performance gap reflecting real modulation [20] (for more details, please refer to [12] and [20]). From (3), we notice that the backscatter rate in the BS mode is controlled by both the circuit elements and the system parameters. Finally, the backscatter bits of U_i in the BS mode is given by

$$R_b^i = B_b^i \hat{\alpha}_i. \quad (4)$$

Therefore, the total transmission bits of the secondary communication system is given by

$$R = \sum_{i=1}^{K} \left(R_h^i + R_a^i + R_b^i\right). \quad (5)$$

III. Optimal Time Allocation

Under the system model given in Section II, we study the optimal time allocation strategy for maximizing the total transmission bits of the secondary communication system. Denote $\boldsymbol{\alpha} = [\alpha_1, \ldots, \alpha_K]$, $\hat{\boldsymbol{\alpha}} = [\hat{\alpha}_1, \ldots, \hat{\alpha}_K]$, $\boldsymbol{t} = [t_1, \ldots, t_K]$, and $\boldsymbol{\tau} = [\tau_1, \tau_2]$. From (5), the optimization problem under the time allocation constraints is formulated as

$$\begin{aligned} \max_{\boldsymbol{\alpha},\hat{\boldsymbol{\alpha}},\boldsymbol{\tau},\boldsymbol{t}} \quad & R\left(\boldsymbol{\alpha}, \hat{\boldsymbol{\alpha}}, \boldsymbol{\tau}, \boldsymbol{t}\right) \\ \text{s.t.} \quad & \text{C1:} \quad \tau_1 + \sum_{i=1}^{K} \alpha_i \leq 1 - \beta \\ & \text{C2:} \quad \tau_2 + \sum_{i=1}^{K} \hat{\alpha}_i + \sum_{i=1}^{K} t_i \leq \beta \\ & \text{C3:} \quad \tau_1, \tau_2 \geq 0 \\ & \text{C4:} \quad \alpha_i, \hat{\alpha}_i, t_i \geq 0 \quad \forall i \end{aligned} \quad \text{(P1)}$$

where C1 guarantees that the summation of the total backscattering time of all CUs in the AB mode and the dedicated EH time should not exceed the primary channel busy time, C2 limits the total time of the BS and HTT modes during the primary channel idle period, C3 and C4 are the non-negative constraints for the time allocation variables.

A. Multiple Cognitive Users Case

In this section, we study the optimal solution for Problem P1 with $K \geq 2$. Before solving Problem P1, we first have the following lemma.

Lemma 1: The objective function R is a jointly concave function of $\boldsymbol{\alpha}$, $\hat{\boldsymbol{\alpha}}$, $\boldsymbol{\tau}$ and $\boldsymbol{t}$.

Proof: Please refer to Appendix A. ∎

With the fact that R is a concave function of $\boldsymbol{\alpha}$, $\hat{\boldsymbol{\alpha}}$, $\boldsymbol{\tau}$, and $\boldsymbol{t}$, and all constraints of Problem P1 are affine, we derive that Problem P1 is a convex optimization problem [29]. There are many standard numerical methods to solve a convex optimization problem. To make the implementation simple, here we adopt the interior-point method [29]. However, we cannot derive any physical insights from the results obtained by this method, especially the combination of working modes in the optimal condition. To study the insights of the proposed transmission mode, we further study a special case, e.g., $K = 1$, in the following section.

B. Single Cognitive User Case

In this section, we study a special case of the system model, where $K = 1$. For the special case, we obtain the combinations of working modes by analyzing the optimal solution.

With $K = 1$, R is simplified as follows:

$$\begin{aligned} R(\alpha_1, \hat{\alpha}_1, \boldsymbol{\tau}, t_1) &= R_h^1 + R_a^1 + R_b^1 \\ &= t_1 W \log_2\left(1 + \frac{\gamma_p^1 \tau_1 + \gamma_h^1 \tau_2}{t_1}\right) \\ &\quad + B_a^1 \alpha_1 + B_b^1 \hat{\alpha}_1 \end{aligned} \tag{6}$$

and the optimization problem is reformulated as

$$\begin{aligned} \max_{\alpha_1, \hat{\alpha}_1, \boldsymbol{\tau}, t_1} \quad & R\big(\alpha_1, \hat{\alpha}_1, \boldsymbol{\tau}, t_1\big) \\ \text{s.t.} \quad & \tau_1 + \alpha_1 \leq 1 - \beta \\ & \tau_2 + \hat{\alpha}_1 + t_1 \leq \beta \\ & \tau_1, \tau_2 \geq 0 \\ & \alpha_1, \hat{\alpha}_1, t_1 \geq 0. \end{aligned} \tag{P2}$$

Denote the optimal solution for Problem P2 as α_1^*, $\hat{\alpha}_1^*$, t_1^*, and $\boldsymbol{\tau}^* = [\tau_1^*, \tau_2^*]$. Before solving Problem P2, we have the following lemma.

Lemma 2: The optimal solution for Problem P2 satisfies

$$\tau_1^* + \alpha_1^* = 1 - \beta \quad \text{and} \quad \tau_2^* + \hat{\alpha}_1^* + t_1^* = \beta.$$

Since $R(\alpha_1, \hat{\alpha}_1, \boldsymbol{\tau}, t_1)$ is an increasing function with respect to α_1 and $\hat{\alpha}_1$, the proof of Lemma 2 can be done by contradiction and is omitted here for simplicity.

To solve Problem P2, we consider two cases following [20], i.e., $\tau_2 = 0$ and $0 < \tau_2 \leq \beta$. If $\tau_2 = 0$, it indicates that U_1 can harvest sufficient energy when the primary channel stays in the busy state and the EH during the primary channel idle period is not necessary. While, if $\tau_2 > 0$, U_1 may harvest energy during both the primary channel busy and idle periods. From Lemma 2, Problem P2 for the case $\tau_2 = 0$ is rewritten as

$$\begin{aligned} \max_{\tau_1, t_1} \quad & R(\tau_1, t_1) \\ \text{s.t.} \quad & 0 \leq \tau_1 \leq 1 - \beta \\ & 0 \leq t_1 \leq \beta \end{aligned} \tag{P3}$$

where $R(\tau_1, t_1) = t_1 W \log_2(1 + [(\gamma_p^1 \tau_1)/t_1]) + B_a^1(1 - \beta - \tau_1) + B_b^1(\beta - t_1)$.

From Lemma 1, we know that Problem P3 is a convex optimization problem. The Lagrangian is given by

$$\begin{aligned} \mathcal{L}(\tau_1, t_1) &= t_1 W \log_2\left(1 + \frac{\gamma_p^1 \tau_1}{t_1}\right) + B_a^1(1 - \beta - \tau_1) \\ &\quad + B_b^1(\beta - t_1) + \mu_1 \tau_1 - \mu_2(\tau_1 - 1 + \beta) \\ &\quad + \nu_1 t_1 - \nu_2(t_1 - \beta) \end{aligned} \tag{7}$$

where μ_i and ν_i, $i = 1, 2$, are the Lagrangian multipliers. From Problem P3, we observe that there exists a solution $\{\tau_1, t_1\}$ satisfying the constraints $0 < \tau_1 < 1 - \beta$ and $0 < t_1 < \beta$, which indicates that strong duality holds since the Slater's condition is satisfied [29]. Hence, Problem P3 can be solved by KKT conditions, which are given by

$$\begin{aligned} \frac{\partial \mathcal{L}}{\partial t_1} &= W \log_2\left(1 + \frac{\gamma_p^1 \tau_1^*}{t_1^*}\right) - W \frac{\frac{\gamma_p^1 \tau_1^*}{t_1^*}}{\ln 2\left(1 + \frac{\gamma_p^1 \tau_1^*}{t_1^*}\right)} \\ &\quad - B_b^1 + \nu_1^* - \nu_2^* \\ &= 0 \end{aligned} \tag{8}$$

$$\begin{aligned} \frac{\partial \mathcal{L}}{\partial \tau_1} &= \frac{W \gamma_p^1}{\ln 2\left(1 + \frac{\gamma_p^1 \tau_1^*}{t_1^*}\right)} - B_a^1 + \mu_1^* - \mu_2^* \\ &= 0 \end{aligned} \tag{9}$$

$$\mu_1^* \tau_1^* = 0 \tag{10}$$

$$\mu_2^*\big(\tau_1^* - 1 + \beta\big) = 0 \tag{11}$$

$$\nu_1^* t_1^* = 0 \tag{12}$$

$$\nu_2^*\big(t_1^* - \beta\big) = 0 \tag{13}$$

where τ_1^*, t_1^*, μ_i^* and ν_i^*, $i = 1, 2$, are the optimal solution for Problem P3. Before analyzing the details of the KKT conditions, we first give Lemma 3 as follows.

Lemma 3: There exists a unique $z^* > 2^{[(B_b^1 + c)/W]}$ satisfies $f(z, c) = 0$, where

$$f(z, c) = z \ln z - \left(1 + \frac{\ln 2(B_b^1 + c)}{W}\right) z + 1$$

and c is a constant.

Proof: Please refer to Appendix B. ∎

Lemma 4: If $[(\ln 2(B_a^1 - B_b^1))/W] < \gamma_p^1$, there exists a unique $z^\dagger > 1$ satisfies $g(z) = \gamma_p^1$, where

$$g(z) = f(z, c = 0) + \frac{\ln 2 B_a^1}{W} z.$$

The proof of Lemma 4 is similar as Proof 2 and is omitted for simplicity.

For the KKT conditions, we first consider the following five cases with $\mu_1^* = 0$, which corresponds to $\tau_1^* \geq 0$.

Case 1: $\mu_2^* > 0$, $\nu_1^* = 0$, and $\nu_2^* = 0$. From (11), we derive that $\tau_1^* = 1 - \beta$. Based on (8), we have the following equation:

$$f(z^*, c) = 0$$

where $z^* = 1 + [(\gamma_p^1 \tau_1^*)/t_1^*]$ is its unique solution with $c = 0$ following Lemma 3. t_1^* is thus expressed as $t_1^* = [(\gamma_p^1 \tau_1^*)/z^* - 1] = [(\gamma_p^1(1-\beta))/z^* - 1]$. This optimal solution indicates that U_1 will not work in the AB mode, but it first enters the BS mode with $\beta - [(\gamma_p^1(1-\beta))/z^* - 1]$ amount of time and then switches to the information transmission phase of the HTT mode. We then analyze the conditions for case 1. Based on $t_1^* \leq \beta$, we have the condition $z^* \geq x^*$, where $x^* = 1 + [(\gamma_p^1(1-\beta))/\beta]$. Moreover, from (9), we have the condition $B_a^1 < [(W\gamma_p^1)/\ln 2z^*]$. The two conditions for case 1 can be combined as $B_a^1 < [(W\gamma_p^1)/(\ln 2z^*)] \leq [(W\gamma_p^1)/\ln 2x^*]$. Note that a similar analysis can be found in [20].

Case 2: $\mu_2^* > 0$, $\nu_1^* = 0$, and $\nu_2^* > 0$. From (11) and (13), we derive that $\tau_1^* = 1 - \beta$ and $t_1^* = \beta$. From the optimal solution, we observe that both AB and BS modes cannot be activated and the secondary communication system works as a WPCN proposed in [8]. The conditions of case 2 are given as follows. We have the following conditions from (8) and (9): $z^+ > z^*$ and $B_a^1 < [(W\gamma_p^1)/\ln 2z^+]$, where z^+ is the unique solution of $f(z, c) = 0$ with $c = \nu_2^* > 0$. We also derive that $z^+ = 1 + [(\gamma_p^1(1-\beta))/\beta] = x^*$. The conditions are combined as $B_a^1 < (W\gamma_p^1/\ln 2x^*) < (W\gamma_p^1/\ln 2z^*)$.

Case 3: $\mu_2^* = 0$, $\nu_1^* = 0$, and $\nu_2^* > 0$. From (13), we derive $t_1^* = \beta$. From (9), we have $\tilde{z} = (W\gamma_p^1/\ln 2B_a^1)$, where $\tilde{z} = 1 + [(\gamma_p^1 \tau_1^*)/t_1^*]$. Hence, we derive $\tau_1^* = [((\tilde{z}-1)\beta)/\gamma_p^1] = [W\beta/(\ln 2B_a^1)] - [\beta/(\gamma_p^1)]$. From the result, we have the following observation. When the primary channel is busy, U_1 first works in the AB mode with $1 - \beta - [W\beta/(\ln 2B_a^1)] + [\beta/(\gamma_p^1)]$ amount of time and then harvests energy with the remaining time. In contrary, the BS mode cannot be activated when the primary channel stays in the idle state. Since $\tau_1^* \leq 1 - \beta$, we have the condition $\tilde{z} \leq x^*$. Furthermore, we also have the condition $\tilde{z} > z^*$ as given in case 2 according to (8). The two conditions are combined as $(W\gamma_p^1/\ln 2x^*) \leq B_a^1 < [(W\gamma_p^1)/\ln 2z^*]$.

Case 4: $\mu_2^* = 0$, $\nu_1^* = 0$ and $\nu_2^* = 0$. According to Lemma 4, if we can find a solution $z^\dagger$ satisfying

$$f(z, c) = \gamma_p^1 - \frac{\ln 2 B_a^1}{W} z \tag{14}$$

with $c = 0$, we have $z^\dagger = z^* = \tilde{z}$. $\{\tau_1^*, t_1^*\}$ can be any values in the feasible domain satisfying $z^\dagger = 1 + [(\gamma_p^1 \tau_1^*)/t_1^*]$. The condition of case 4 can be given as $B_a^1 = [(W\gamma_p^1)/\ln 2z^*]$. If there does not exist a solution for (14), this case does not exist.

Case 5: $\mu_2^* = 0$, $\nu_1^* > 0$ and $\nu_2^* = 0$. From (12), we have $t_1^* = 0$, which indicates that the information transmission phase of the HHT mode cannot work. Hence, the EH is not necessary, i.e., $\tau_1^* = 0$. From the optimal solution, we know that whether the primary channel is busy or idle, U_1 always stays in the BackCom mode. The condition for this case is given as follows. From (9), we have $B_a^1 = (W\gamma_p^1/\ln 2\check{z})$ and $\check{z} < z^*$, where $\check{z}$ is the optimal solution of $f(z, c) = 0$ with $c = -\nu_1^* < 0$. Hence, the condition for this case is given as $B_a^1 > (W\gamma_p^1/\ln 2z^*)$.

Next, we consider the following case with $\mu_1^* > 0$, which corresponds to $\tau_1^* = 0$ according to (10).

Case 6: $\mu_2^* = 0$, $\nu_1^* \geq 0$ and $\nu_2^* = 0$. Since $\tau_1^* = 0$, U_1 cannot harvest any energy from the PT. Hence, U_1 cannot transmit any data, i.e., $t_1^* = 0$. This case is similar as case 5, i.e., the HTT mode cannot be activated and U_1 works in the BackCom mode over the whole block. The condition for this case is given as follows. We also denote $\check{z}$ as the optimal solution of $f(z, c) = 0$ with $c = -\nu_1^* \leq 0$. From (9), we have $B_a^1 > [(W\gamma_p^1)/\ln 2\check{z}]$ and $\check{z} \leq z^*$. The condition is thus given as $B_a^1 > [(W\gamma_p^1)/\ln 2z^*]$. Hence, case 5 and case 6 can be combined.

Note that under $\mu_1^* \geq 0$, there are still other combinations of the Lagrangian multipliers. However, the other combinations make the KKT conditions contradict with each other. Hence, we do not discuss the cases corresponding to the unmentioned combinations here.

We then consider Problem P2 with $\tau_2 > 0$. From Lemma 2, Problem P2 is recast as Problem P4

$$\begin{aligned} \max_{\boldsymbol{\tau}, t_1} \ & R(\boldsymbol{\tau}, t_1) \\ \text{s.t.} \ & \tau_1 \leq 1 - \beta \\ & \tau_2 + t_1 \leq \beta \\ & \tau_2, t_1 > 0, \ \tau_1 \geq 0 \end{aligned} \tag{P4}$$

where $R(\boldsymbol{\tau}, t_1) = t_1 W \log_2(1 + [(\gamma_p^1 \tau_1 + \gamma_h^1 \tau_2)/t_1]) + B_a^1(1 - \beta - \tau_1) + B_b^1(\beta - t_1 - \tau_2)$. Problem P4 is also a convex optimization problem following Lemma 1. Before solving Problem P4, we first derive the optimal relationship between τ_2 and t_1 with given τ_1. Let $\bar{t} = \tau_2 + t_1 \leq \beta$. Hence, Problem P4 is recast as Problem P5, which is given by

$$\begin{aligned} \max_{\tau_2, t_1} \ & R(\tau_2, t_1) \\ \text{s.t.} \ & t_1 + \tau_2 = \bar{t} \\ & t_1, \tau_2 > 0. \end{aligned} \tag{P5}$$

Problem P5 can also be solved by KKT conditions and its Lagrangian is given as

$$\begin{aligned} \mathcal{L}(\tau_2, t_1, \zeta) = & \, t_1 W \log_2\left(1 + \frac{\gamma_p^1 \tau_1 + \gamma_h^1 \tau_2}{t_1}\right) \\ & + B_a^1(1 - \beta - \tau_1) + B_b^1(\beta - t_1 - \tau_2) \\ & - \zeta(t_1 + \tau_2 - \bar{t}) \end{aligned}$$

where ζ is the Lagrangian multiplier. The KKT conditions are given by

$$\begin{aligned} \frac{\partial \mathcal{L}}{\partial \tau_2} &= W \frac{\gamma_h^1}{\ln 2\left(1 + \frac{\gamma_p^1 \tau_1^* + \gamma_h^1 \tau_2^*}{t_1^*}\right)} - B_b^1 - \zeta^* \\ &= 0 \end{aligned} \tag{15}$$

$$\frac{\partial \mathcal{L}}{\partial t_1} = W\log_2\left(1+\frac{\gamma_p^1\tau_1^*+\gamma_h^1\tau_2^*}{t_1^*}\right) - W\frac{\frac{\gamma_p^1\tau_1^*+\gamma_h^1\tau_2^*}{t_1^*}}{\ln 2\left(1+\frac{\gamma_p^1\tau_1^*+\gamma_h^1\tau_2^*}{t_1^*}\right)}$$

$$-B_b^1-\zeta^*=0 \tag{16}$$

$$\zeta^*\left(t_1^*+\tau_2^*-\bar{t}\right)=0. \tag{17}$$

Lemma 5 is given here for the following discussions of the KKT conditions.

Lemma 5: There exists a unique $\bar{z}>1$ satisfies $h(z)=b$ $(b>0)$, where

$$h(z)=z\ln z-z+1.$$

The proof of Lemma 5 is also omitted for simplicity.

From (15) and (16), we derive τ_2^* and t_1^*, which are given by

$$\tau_2^*=\frac{\bar{z}\bar{t}-\bar{t}-\gamma_p^1\tau_1}{\bar{z}-1+\gamma_h^1} \tag{18}$$

$$t_1^*=\frac{\bar{t}\gamma_h^1+\gamma_p^1\tau_1}{\bar{z}-1+\gamma_h^1} \tag{19}$$

where $\bar{z}>1$ is the unique solution of $h(z)=\gamma_h^1$. With (18) and (19), we have $R(\bar{t},\tau_1)=[(\bar{t}\gamma_h^1+\gamma_p^1\tau_1)/(\bar{z}-1+\gamma_h^1)]W\log_2\bar{z}+B_a^1(1-\beta-\tau_1)+B_b^1(\beta-\bar{t})=([\gamma_h^1/(\bar{z}-1+\gamma_h^1)]W\log_2\bar{z}-B_b^1)\bar{t}+([\gamma_p^1/(\bar{z}-1+\gamma_h^1)]W\log_2\bar{z}-B_a^1)\tau_1+B_a^1(1-\beta)+B_b^1\beta$. Problem P4 is reformulated as

$$\begin{aligned}\max_{\tau_1,\bar{t}}\ & R\left(\bar{t},\tau_1\right)\\ \text{s.t.}\ & 0<\bar{t}\le\beta\\ & 0\le\tau_1\le 1-\beta.\end{aligned} \tag{P6}$$

Denote the optimal solution for Problem P6 as τ_1^* and $\bar{t}^*$. To solve Problem P6, we consider the following two cases by taking $\bar{t}>0$ into account.

Case 7: $[\gamma_h^1/(\bar{z}-1+\gamma_h^1)]W\log_2\bar{z}>B_b^1$ and $[\gamma_p^1/(\bar{z}-1+\gamma_h^1)]W\log_2\bar{z}\ge B_a^1$. In this case, we derive that $\bar{t}^*=\beta$ and $\tau_1^*=1-\beta$. Hence, the other optimal variables for Problem P4 are given as $\tau_2^*=[(\bar{z}\beta-\beta-\gamma_p^1(1-\beta))/(\bar{z}-1+\gamma_h^1)]$ and $t_1^*=[(\beta\gamma_h^1+\gamma_p^1(1-\beta))/(\bar{z}-1+\gamma_h^1)]$. For this case, the secondary communication system only works in the HTT mode. Since $0<\tau_2<\beta$, we further have the condition $\bar{z}>1+[(\gamma_p^1(1-\beta))/\beta]$.

Case 8: $[\gamma_h^1/(\bar{z}-1+\gamma_h^1)]W\log_2\bar{z}>B_b^1$ and $[\gamma_p^1/(\bar{z}-1+\gamma_h^1)]W\log_2\bar{z}<B_a^1$. In this case, we derive that $\bar{t}^*=\beta$ and $\tau_1^*=0$. Hence, the other optimal variables for Problem P4 are given as $\tau_2^*=[(\bar{z}\beta-\beta)/(\bar{z}-1+\gamma_h^1)]$ and $t_1^*=[(\beta\gamma_h^1)/(\bar{z}-1+\gamma_h^1)]$. For this case, U_1 works in the AB mode when the primary channel stays in the busy state and works in the HTT mode when the primary channel stays in the idle state.

The optimal solutions of Problem P2 is summarized in Table I. The optimal combination of working modes corresponds to the result that achieves the maximum throughput.

IV. Benchmark Scheme

In this section, we present a benchmark scheme where only the HTT mode is adopted. For the benchmark, when the primary channel stays in the busy state, the CUs only harvest energy from the PT simultaneously. When the primary channel stays in the idle state, the secondary communication system works as a stand-alone WPCN [8], [22]. Since the BackCom mode is not available, we let $\boldsymbol{\alpha}=0$ and $\hat{\boldsymbol{\alpha}}=0$ ("=" denotes the component-wise equality). R is thus recast as

$$R(\boldsymbol{\tau},\boldsymbol{t})=\sum_{i=1}^{K}t_iW\log_2\left(1+\frac{\gamma_p^i\tau_1+\gamma_h^i\tau_2}{t_i}\right) \tag{20}$$

and Problem P1 is recast as

$$\begin{aligned}\max_{\boldsymbol{\tau},\boldsymbol{t}}\ & R(\boldsymbol{\tau},\boldsymbol{t})\\ \text{s.t.}\ & \tau_1\le 1-\beta\\ & \tau_2+\sum_{i=1}^{K}t_i\le\beta\\ & \tau_1,\tau_2,t_i\ge 0.\end{aligned} \tag{P7}$$

Taking the method proposed in [8], we have

$$\tau_1^*=1-\beta$$

$$\tau_2^*=\max\left\{0,\frac{\beta\left(z^\ddagger-1\right)-\sum_{j=1}^{K}\gamma_p^j(1-\beta)}{z^\ddagger-1+\sum_{j=1}^{K}\gamma_h^j}\right\}$$

$$t_i^*=\frac{\left(\beta-\tau_2^*\right)\left(\gamma_p^i(1-\beta)+\gamma_h^i\tau_2^*\right)}{\sum_{j=1}^{K}\gamma_p^j(1-\beta)+\sum_{j=1}^{K}\gamma_h^j\tau_2^*},\ i=1,\ldots,K$$

where $z^\ddagger>1$ is the unique solution for $h(z)=\sum_{i=1}^{K}\gamma_h^i$.

TABLE I
Optimal Solution of Problem P2

Condition		Optimal solution
$\tau_2^*=0$	$B_a^1<\frac{W\gamma_p^1}{\ln 2z^*}\le\frac{W\gamma_p^1}{\ln 2x^*}$	$\tau_1^*=1-\beta,\ t_1^*=\frac{\gamma_p^1(1-\beta)}{z^*-1}$
	$B_a^1<\frac{W\gamma_p^1}{\ln 2x^*}<\frac{W\gamma_p^1}{\ln 2z^*}$	$\tau_1^*=1-\beta,\ t_1^*=\beta$
	$\frac{W\gamma_p^1}{\ln 2x^*}\le B_a^1<\frac{W\gamma_p^1}{\ln 2z^*}$	$\tau_1^*=\frac{W\beta}{\ln 2B_a^1}-\frac{\beta}{\gamma_p^1},\ t_1^*=\beta$
	$B_a^1>\frac{W\gamma_p^1}{\ln 2z^*}$	$\tau_1^*=0,\ t_1^*=0$
	$B_a^1=\frac{W\gamma_p^1}{\ln 2z^*}$	Any feasible values
$\tau_2^*>0$	$\frac{\gamma_h^1}{\bar{z}-1+\gamma_h^1}W\log_2\bar{z}>B_b^1$, $\frac{\gamma_p^1}{\bar{z}-1+\gamma_h^1}W\log_2\bar{z}\ge B_a^1$ $\bar{z}>1+\frac{\gamma_p^1(1-\beta)}{\beta}$	$\tau_1^*=1-\beta,\ t_1^*=\frac{\beta\gamma_h^1+\gamma_p^1(1-\beta)}{\bar{z}-1+\gamma_h^1}$ $\tau_2^*=\frac{\bar{z}\beta-\beta-\gamma_p^1(1-\beta)}{\bar{z}-1+\gamma_h^1}$
	$\frac{\gamma_h^1}{\bar{z}-1+\gamma_h^1}W\log_2\bar{z}>B_b^1$, $\frac{\gamma_p^1}{\bar{z}-1+\gamma_h^1}W\log_2\bar{z}<B_a^1$	$\tau_1^*=0,\ t_1^*=\frac{\beta\gamma_h^1}{\bar{z}-1+\gamma_h^1}$ $\tau_2^*=\frac{\bar{z}\beta-\beta}{\bar{z}-1+\gamma_h^1}$

V. Numerical Results

In this section, numerical simulations are conducted to evaluate the performance of the proposed hybrid HTT-BackCom mode. We also present the numerical results of the benchmark for comparison. In our numerical experiments, the PT transmits signals at 915 MHz with 6 MHz bandwidth, while the PB transmits signals at 2.4 GHz with 20 MHz bandwidth. The antenna gain of each CU is set as 1.8 dBi, the antenna gains of other devices are set as 6 dBi, and the reflection coefficients of the BS mode are set as $\Gamma_0=1$ and $\Gamma_1=-1$, respectively. The scattering efficiency s causes a power loss of 1.1 dB.

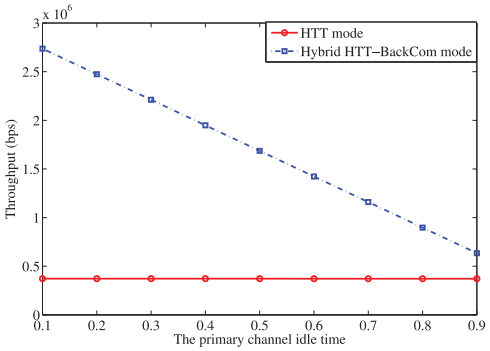

Fig. 3. Throughput versus primary channel idle time.

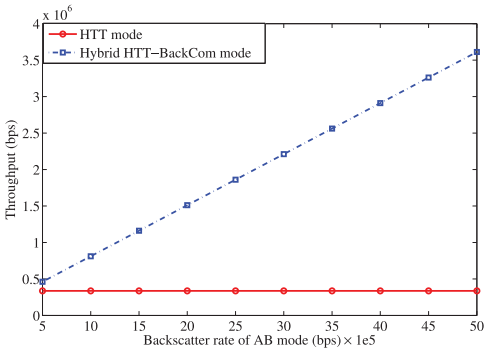

Fig. 4. Throughput versus AB mode's rate.

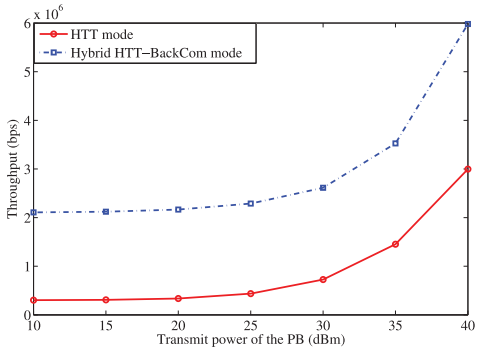

Fig. 5. Throughput versus PB's transmit power.

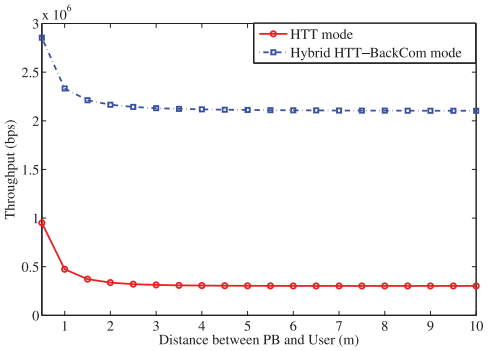

Fig. 6. Throughput versus distance between PB and user.

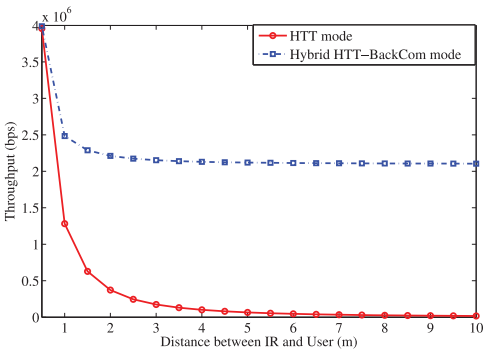

Fig. 7. Throughput versus distance between IR and user.

Unless otherwise stated, we set $P_p = 17$ kW, $P_h = 20$ dBm, $d_p^i = 1$ km, $d_h^i = 1.5$ m, $d_u^i = 2$ m, $\beta = 0.3$, $\eta^i = 0.6$, $\xi = -5$ dB, $\sigma^2 = -20$ dBm, and $B_a^i = 3$ Mb/s. We show that our proposed hybrid HTT-BackCom mode outperforms the traditional HTT mode in terms of system throughput.

Fig. 3 shows the throughput versus the primary channel idle time. From Fig. 3, we can see that the proposed hybrid HTT-BackCom mode leads to a larger throughput than the HTT mode. This can be explained as follows. Under the given parameters, U_1 always works in the AB mode when the primary channel stays in the busy state and works in the HTT mode when the primary channel stays in the idle state for the proposed hybrid HTT-BackCom mode. Moreover, the AB mode's backscatter rate is larger than the HTT mode's transmission rate. We also see that the throughput achieved by the proposed hybrid HTT-BackCom mode decreases with the increase of the primary channel idle time β. It is because as β increases, the time for the AB mode reduces and the time for the HTT mode increases, which reduces the throughput. In Fig. 4, we vary the AB mode's backscatter rate to evaluate the throughput. It is obvious that the AB mode affects the throughput significantly.

Fig. 5 shows the throughput of the secondary communication system versus the PB's transmit power. We observe that the throughput is an increasing function with respect to the PB's transmit power for both the proposed hybrid HTT-BackCom mode and HTT mode. As the transmit power increases, the throughput increases first slowly and then fast. This can be explained as follows. The rates of both BS and HTT modes increase with the increase of the PB's transmit power. When the PB's transmit power is low, U_1 works in the HTT mode for information transmission during the primary channel idle period. When the PB's transmit power exceeds a threshold (e.g., 30 dBm), U_1 works in the BS mode for information backscattering and the rate of the BS mode increases fast.

Figs. 6 and 7 show the throughput versus the distances between the PB and U_1 and between the IR and U_1, respectively. It is obvious that as the distances increase, the throughput reduces fast first and then slowly. The observation in Fig. 6 is because the energy harvested from the PB first reduces significantly and then tends to be negligible. In Fig. 7, when the distance $d_u^1 = 0.5$ m, the throughput of the proposed and benchmark modes is almost the same. It is because in this case the HTT mode dominates the throughput for the proposed mode.

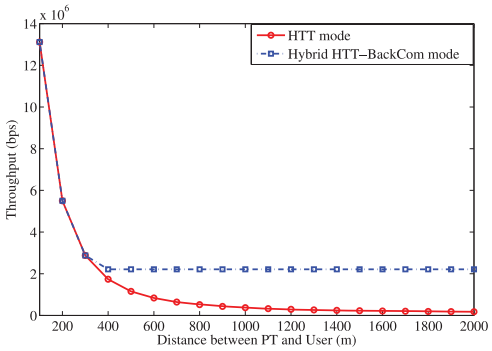

Fig. 8. Throughput versus distance between PT and user.

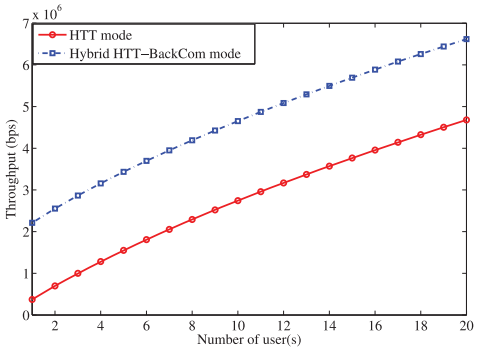

Fig. 9. Throughput versus number of user(s).

Fig. 8 depicts the curves of the throughput versus the distance between the PT and U_1. Similar with Figs. 6 and 7, the throughput reduces as the distance increases. When the distance is small, the throughput achieved by the proposed hybrid HTT-BackCom mode and benchmark mode is the same since U_1 only works in the HTT mode for the proposed mode. When the distance exceeds a threshold (e.g., 300 m), U_1 first works in the HTT mode and then in the AB mode due to the reduce of harvested energy.

Fig. 9 investigates the throughput versus the number of users. The throughput of the proposed and benchmark modes increases with the number of users. The reason is that, as the number of users increases, the total energy harvested by the users increases but the allocated time of each user for information transmission reduces, which results in a higher transmit power at the users in the HTT mode. Moreover, it is observed that the throughput of the proposed mode is larger than that of the benchmark mode.

VI. Conclusion

In this paper, we have proposed a novel hybrid HTT-BackCom mode in CWPCNs for IoT, where the CUs in the secondary communication system work in the HTT mode, the AB mode or the BS mode. The signal from the PT and the signal from the PB serve as the excitation signals for the AB mode and BS mode, respectively, while the PT and PB are both the energy sources for the HTT mode. Under the proposed hybrid mode, we have investigated the secondary communication system throughput maximization problem by finding the optimal time allocation between the AB mode and EH when the primary channel stays in the busy state and that between the BS mode and the HTT mode when the primary channel stays in the idle state. To be specific, we have derived the optimal solution in closed-form for a signal CU case, and obtained the optimal combination of the working modes. Numerical results have confirmed that our proposed hybrid HTT-BackCom achieves a higher throughput than the traditional HTT mode, which shows the advantages of combining the HTT and BackCom modes. For the future work, we will consider to employ multiantenna techniques at the PB to further improve the system performance.

Appendix A
Proof of Lemma 1

We first prove $R_h^i, \forall i$ is a jointly concave function of $\boldsymbol{\alpha}$, $\hat{\boldsymbol{\alpha}}$, $\boldsymbol{\tau}$, and $\boldsymbol{t}$. Define $f_i(\boldsymbol{\alpha}, \hat{\boldsymbol{\alpha}}, \boldsymbol{\tau}) = W \log_2(1 + \gamma_p^i(\sum_{j\neq i} \alpha_j + \tau_1) + \gamma_h^i(\sum_{j\neq i} \hat{\alpha}_j + \tau_2))$, where f_i is a concave function of $\boldsymbol{\alpha}$, $\hat{\boldsymbol{\alpha}}$, and $\boldsymbol{\tau}$. We observe that R_h^i is a perspective function of $f_i(\boldsymbol{\alpha}, \hat{\boldsymbol{\alpha}}, \boldsymbol{\tau})$ [29]. Due to that the perspective operation preserves concavity, we can derive that R_i^h is a jointly concave function of $\boldsymbol{\alpha}$, $\hat{\boldsymbol{\alpha}}$, $\boldsymbol{\tau}$, and $\boldsymbol{t}$. Then, we can easily find that R_a^i and R_b^i are also concave functions of $\boldsymbol{\alpha}$, $\hat{\boldsymbol{\alpha}}$, $\boldsymbol{\tau}$, and $\boldsymbol{t}$. R is thus a concave function of $\boldsymbol{\alpha}$, $\hat{\boldsymbol{\alpha}}$, $\boldsymbol{\tau}$, and $\boldsymbol{t}$ since it is the summation of R_h^i, R_a^i, and R_b^i.

Appendix B
Proof of Lemma 3

The first and second derivatives of $f(z, c)$ are given by

$$\frac{\partial f(z,c)}{\partial z} = \ln z - \ln 2^{\frac{B_b^1 + c}{W}} \tag{21}$$

$$\frac{\partial^2 f(z,c)}{\partial z^2} = \frac{1}{z}. \tag{22}$$

From (21) and (22), we derive the minimum of $f(z, c)$ is achieved at $z = 2^{[(B_b^1+c)/W]}$ with $f(z = 2^{[(B_b^1+c)/W]}, c) = 1 - 2^{[(B_b^1+c)/W]} < 0$, and $f(z, c)$ is an increasing function with $z > 2^{[(B_b^1+c)/W]}$. Moreover, we have

$$\lim_{z\to+\infty} f(z,c) > 0. \tag{23}$$

Hence, we derive that there is a unique solution for $f(z, c) = 0$ with $z > 2^{[(B_b^1+c)/W]}$.

References

[1] S. Verma, Y. Kawamoto, Z. Fadlullah, H. Nishiyama, and N. Kato, "A survey on network methodologies for real-time analytics of massive IoT data and open research issues," *IEEE Commun. Surveys Tuts.*, vol. 19, no. 3, pp. 1457–1477, 3rd Quart., 2017.

[2] W. Liu, K. Huang, X. Zhou, and S. Durrani, "Next generation backscatter communication: Theory and applications," *IEEE Wireless Commun.*, to be published. [Online]. Available: https://arxiv.org/abs/1701.07588.pdf

[3] Y. Kawamoto *et al.*, "A feedback control-based crowd dynamics management in IoT system," *IEEE Internet Things J.*, vol. 4. no. 5, pp. 1466–1476, Oct. 2017.

[4] P. Ramezani and A. Jamalipour, "Toward the evolution of wireless powered communication networks for the future Internet of Things," *IEEE Netw.*, vol. 31, no. 6, pp. 62–69, Nov./Dec. 2017.

[5] H. Kawabata, K. Ishibashi, S. Vuppala, and G. T. F. de Abreu, "Robust relay selection for large-scale energy-harvesting IoT networks," *IEEE Internet Things J.*, vol. 4, no. 2, pp. 384–392, Apr. 2017.

[6] X. Lu, P. Wang, D. Niyato, D. I. Kim, and Z. Han, "Wireless networks with RF energy harvesting: A contemporary survey," *IEEE Commun. Surveys Tuts.*, vol. 17, no. 2, pp. 757–789, 2nd Quart., 2015.

[7] B. Lyu, C. You, Z. Yang, and G. Gui, "The optimal control policy for RF-powered backscatter communication networks," *IEEE Trans. Veh. Technol.*, vol. 67. no. 3, pp. 2804–2808, Mar. 2018.

[8] H. Ju and R. Zhang, "Throughput maximization in wireless powered communication networks," *IEEE Trans. Wireless Commun.*, vol. 13, no. 1, pp. 418–428, Jan. 2014.

[9] H. Ju and R. Zhang, "Optimal resource allocation in full-duplex wireless-powered communication network," *IEEE Trans. Commun.*, vol. 62, no. 10, pp. 3528–3540, Oct. 2014.

[10] H. Ju and R. Zhang, "User cooperation in wireless powered communication networks," in *Proc. GLOBECOM*, Austin, TX, USA, Dec. 2014, pp. 1430–1435.

[11] H. Chen, Y. Li, J. L. Rebelatto, B. F. Uchôa-Filho, and B. Vucetic, "Harvest-then-cooperate: Wireless-powered cooperative communications," *IEEE Trans. Signal Process.*, vol. 63, no. 7, pp. 1700–1711, Apr. 2015.

[12] J. Kimionis, A. Bletsas, and J. N. Sahalos, "Increased range bistatic scatter radio," *IEEE Trans. Commun.*, vol. 62, no. 3, pp. 1091–1104, Mar. 2014.

[13] V. Liu *et al.*, "Ambient backscatter: Wireless communication out of thin air," in *Proc. SIGCOMM*, Hong Kong, Aug. 2013, pp. 39–50.

[14] A. N. Parks, A. Liu, S. Gollakota, and J. R. Smith, "Turbocharging ambient backscatter communication," in *Proc. SIGCOMM*, Chicago, IL, USA, Aug. 2014, pp. 619–630.

[15] X. Lu *et al.*, "Ambient backscatter networking: A novel paradigm to assist wireless powered communications," *IEEE Wireless Commun.*, to be published, doi: 10.1109/MWC.2017.1600398.

[16] B. Lyu, Z. Yang, G. Gui, and Y. Feng, "Throughput maximization in backscatter assisted wireless powered communication networks," *IEICE Trans. Fundamentals*, vol. E100-A, no. 6, pp. 1353–1357, Jun. 2017.

[17] B. Lyu, Z. Yang, and G. Gui, "Throughput maximization in backscatter assisted wireless powered communication networks with battery constraint," in *Proc. WCSP*, Nanjing, China, Oct. 2017, pp. 1–5.

[18] B. Lyu, Z. Yang, G. Gui, and Y. Feng, "Wireless powered communication networks assisted by backscatter communication," *IEEE Access*, vol. 5, pp. 7254–7262, 2017, doi: 10.1109/ACCESS.2017.2677521.

[19] B. Lyu, Z. Yang, G. Gui, and H. Sari, "Optimal time allocation in backscatter assisted wireless powered communication networks," *Sensors*, vol. 17, no. 6, 2017, Art. no. E1258, doi: 10.3390/s17061258.

[20] S. H. Kim and D. I. Kim, "Hybrid backscatter communication for wireless-powered heterogeneous networks," *IEEE Trans. Wireless Commun.*, vol. 16, no. 10, pp. 6557–6570, Oct. 2017.

[21] A. A. Khan, M. H. Rehmani, and A. Rachedi, "Cognitive-radio-based Internet of Things: Applications, architectures, spectrum related functionalities, and future research directions," *IEEE Wireless Commun.*, vol. 24, no. 3, pp. 17–25, Jun. 2017.

[22] S. Lee and R. Zhang, "Cognitive wireless powered network: Spectrum sharing models and throughput maximization," *IEEE Trans. Cogn. Commun. Netw.*, vol. 1, no. 3, pp. 335–346, Sep. 2015.

[23] D. Zhang *et al.*, "Utility-optimal resource management and allocation algorithm for energy harvesting cognitive radio sensor networks," *IEEE J. Sel. Areas Commun.*, vol. 34, no. 12, pp. 3552–3565, Dec. 2016.

[24] D. T. Hoang, D. Niyato, P. Wang, D. I. Kim, and Z. Han, "The tradeoff analysis in RF-powered backscatter cognitive radio networks," in *Proc. IEEE GLOBECOM*, Washington, DC, USA, Dec. 2016, pp. 1–6.

[25] D. T. Hoang, D. Niyato, P. Wang, and D. I. Kim, "Optimal time sharing in RF-powered backscatter cognitive radio networks," in *Proc. IEEE Int. Conf. Commun.*, Paris, France, May 2017, pp. 1–6.

[26] P. Zhang and D. Ganesan, "Enabling bit-by-bit backscatter communication in severe energy harvesting environment," in *Proc. NSDI*, Seattle, WA, USA, Apr. 2014, pp. 345–357.

[27] FCC, *New Policies for Part 15 Devices*, *TCBC Workshop*, 2005.

[28] B. Kellogg, V. Talla, S. Gollakota, and J. R. Smith, "Passive Wi-Fi: Bringing low power to Wi-Fi transmissions," in *Proc. NSDI*, Santa Clara, CA, USA, Mar. 2016, pp. 151–164.

[29] S. Boyd and L. Vandenberghe, *Convex Optimization*. Cambridge, U.K.: Cambridge Univ. Press, 2004.

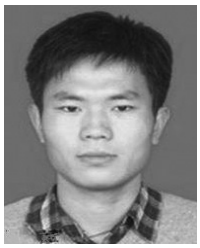

Bin Lyu received the B.E. degree in electronic and information engineering from the Nanjing University of Posts and Telecommunications, Nanjing, China, in 2013, where he is currently pursuing the Ph.D. degree in signal and information processing.

His current research interests include wireless power transfer and backscatter communication.

Haiyan Guo received the B.E. and Ph.D. degrees in signal and information processing from the Nanjing University of Posts and Telecommunications (NUPT), Nanjing, China, in 2005 and 2011, respectively.

She is an Assistant Professor with NUPT. From 2013 to 2014, she was a Post-Doctoral Research Fellow with Southeast University, Nanjing. Her current research interests include physical-layer security and speech signal processing.

Zhen Yang received the B.E. and M.E. degrees from the Nanjing University of Posts and Telecommunications (NUPT), Nanjing, China, in 1983 and 1988, respectively, and the Ph.D. degree from Shanghai Jiao Tong University, Shanghai, China, in 1999, all in electrical engineering.

He was initially a Lecturer with NUPT in 1983, where he became an Associate Professor in 1995 and then a Full Professor in 2000. He was a Visiting Scholar with Bremen University, Bremen, Germany, from 1992 to 1993, and an Exchange Scholar with the University of Maryland at College Park, College Park, MD, USA, in 2003. He has authored or co-authored over 200 papers in academic journals and conferences. His current research interests include various aspects of signal processing and communication, such as communication systems and networks, cognitive radio, spectrum sensing, speech and audio processing, compressive sensing, and wireless communication.

Dr. Yang is currently the Vice Chairman of the Chinese Institute of Communications, a Fellow of the Chinese Institute of Communications, and the Vice Director of the Editorial Board of the *Journal on Communications*. He was the Chairman of the Jiangsu Institute of Communications from 2010 to 2015 and the Chair of the Asian Pacific Communication Conference Steering Committee from 2013 to 2014.

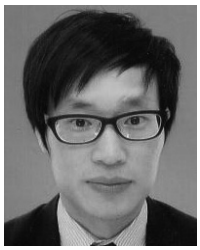

Guan Gui (GS'08–M'11–SM'17) received the Dr.Eng. degree in information and communication engineering from the University of Electronic Science and Technology of China, Chengdu, China, in 2011.

From 2009 to 2012, with the financial support of the China Scholarship Council and the Global Center of Education of Tohoku University, Sendai, Japan, he joined the Wireless Signal Processing and Network Laboratory (Prof. Adachi's Laboratory), Department of Communications Engineering, Graduate School of Engineering, Tohoku University, as a Research Assistant, as well as a Post-Doctoral Research Fellow, respectively, where he was supported by the Japan Society for the Promotion of Science Fellowship as a Post-Doctoral Research Fellow from 2012 to 2014. From 2014 to 2015, he was an Assistant Professor with the Department of Electronics and Information System, Akita Prefectural University, Akita, Japan. Since 2015, he has been a Professor with the Nanjing University of Posts and Telecommunications, Nanjing, China. His current research interests include multidimensional system control, super-resolution radar imaging, adaptive filter, compressive sensing, sparse dictionary designing, channel estimation, and advanced wireless techniques.

Dr. Gui was a recipient of the IEEE International Conference on Communications Best Paper Award and IEEE Vehicular Technology Conference (VTC-Spring) Best Student Paper Award in 2014. He has been an Associate Editor of Wiley's *Journal of Security and Communication Networks* since 2012.